

# Effect of Paraboloidal Dish Structure on the Wind near a Cavity Receiver

S. Paitoonsurikarn and K. Lovegrove

Centre for Sustainable Energy Systems,  
Department of Engineering,  
Australian National University,  
Canberra ACT 0200,  
AUSTRALIA

E-mail: [sawat.paitoonsurikarn@anu.edu.au](mailto:sawat.paitoonsurikarn@anu.edu.au)

## Abstract

*In some cases, convection heat transfer is a major source of thermal loss from a cavity receiver used in a solar dish application. As indicated in the previous study (Paitoonsurikarn et al, 2004), the presence of the wind can greatly affect the magnitude of the convection loss. However, the real effect at a cavity aperture also depends on the interaction between the wind and the dish structure.*

*The present simulation investigates the relation between the magnitude of the freestream wind and that of the wind immediate to the cavity aperture at various wind directions. The configuration of the dish used in the study is that of the 20 m<sup>2</sup> dish currently used in the solar ammonia thermochemical demonstration plant at the ANU. The incidence angle is varied azimuthally, and ranges from -90 degree to 90 degree, corresponding to the wind normally incident on the back of the receiver and the back of the dish, respectively.*

*It is found that the near-aperture velocity is the greatest when the incidence angle is equal to 0 degree, i.e. where the wind is parallel to the aperture plane. Interestingly, the near-aperture velocity magnitude versus the wind direction obviously shows a symmetrical behaviour.*

*Simple correlations to estimate the magnitudes of the normal and parallel velocity components at the aperture from the free-stream wind speed and direction are proposed. The present results could be employed in conjunction with a combined convection correlation for convection loss prediction in the future work.*

## 1. INTRODUCTION

In the solar dish application, convective heat transfer is one of the major modes of energy loss occurring at open-cavity thermal receivers. In previous work (e.g. Paitoonsurikarn & Lovegrove, 2003; Taumoefolau et al, 2004; Paitoonsurikarn et al, 2004), various physical aspects of convective heat transfers, both free and combined modes, have been discussed with an emphasis laid upon the former. Correlation for predicting the free convection loss has also been proposed.

Generally, in the combined convection mode, there is a complex interaction between the wind-induced and the buoyancy-induced flows at the receiver aperture. It was found in the numerical simulations that the magnitude and the direction of the wind can greatly affect the amount of convection loss. In most cases, the magnitude of the heat loss is higher for the case of wind parallel to the aperture plane than that for the case of the head-on wind. This finding is in a good agreement with the conclusion in the experimental work by Ma (1993).

For the combined convection loss prediction, Taumoefolau (2004) proposed the empirical correlation based on the experimental data of the model receiver. His correlation explicitly includes the effect of the wind direction via the multiplication of the function  $g(i)$  to the dimensionless heat transfer coefficient, i.e. the Nusselt number (Nu), where  $i$  is the wind incidence angle. The range of the incidence angle is from 0 deg to 90 deg, corresponding to the cases of parallel wind and head-on wind, respectively.

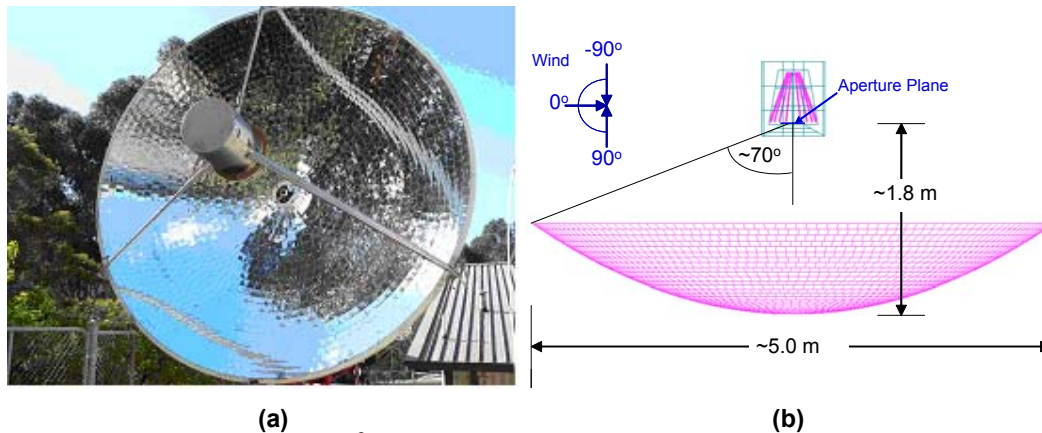


Figure 1 (a) The ANU 20 m<sup>2</sup> Dish and the Solar Receiver/Reactor and (b) Schematic.

Nonetheless, to the author's best knowledge, so far the previous investigations have been undertaken regardless of the dish structure, which can interact with the freestream wind, and drastically affects the wind pattern in the vicinity of the receiver. Therefore, it is of a primary interest in the present work to investigate this effect in detail.

## 2. PROBLEM FORMULATION

The dish-receiver under consideration is essentially derived from the ANU 20 m<sup>2</sup> dish and the receiver/reactor currently used in the solar thermochemical demonstration plant at the Australian National University. Figure 1a shows a photo of the actual system.

Figure 1b illustrates the system with approximate dimensions. The 20 m<sup>2</sup> dish has an aperture diameter of 5.0 m, a focal length of 1.8 m, and a rim angle of approximately 70 deg. The receiver consists of a frustum cavity with an aperture diameter of 0.2 m. In front of the cavity is also a frustum-shaped shield, which makes the aperture plane situated beyond the cylindrical outer casing of the receiver as shown.

The commercial CFD software package, Fluent 6.0 (Fluent Inc., 2002), was employed in the 3D simulation of the wind. Figure 2a shows the schematic of the typical grid system used. It consists of a virtual wind tunnel with the cross-sectional area of 30 m x 30 m. The symmetrical boundary condition was assigned to the tunnel wall, so that it functions as the zero frictional wall to the flow. The dish-receiver system is located near the middle section of the tunnel, and the distances from the tunnel inlet and outlet to the aperture plane are equal to 75 m and 105 m, respectively. Figure 2b shows the

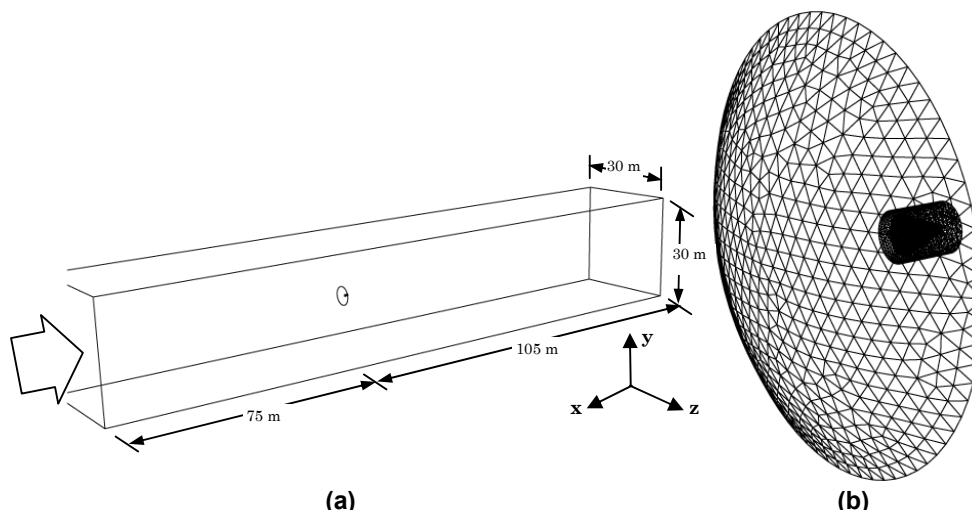


Figure 2 Three-Dimensional Grid Employed in the Simulations: (a) Schematic and (b) Dish & Receiver Close-up.

close-up of the grid construction of the dish-receiver unit.

The dish is oriented facing the horizon. The dish's azimuthal position is adjusted accordingly to vary the wind incidence angle, ranging from -90 deg to 90 deg (cf. Figure 1b). The range of freestream wind speed under study is 0-20 m/s. The heat transfer is not considered herein, so that the temperature of the entire flow system is specified at the ambient condition, i.e., 300 K.

More details of the numerical scheme used can be found in the previous paper (Paitoonsurikarn & Lovegrove, 2003).

### 3. RESULTS AND DISCUSSION

Figure 3 shows the vector plots of an instantaneous velocity field on the middle horizontal cross-section of the wind tunnel. The freestream wind flows from left to right with a speed of 5 m/s.

It is evident that the dish effectively reduces the wind speed near the receiver at all angles of incidence, except for  $i=0$  deg, i.e. for the case of parallel wind. At the same time, there are formations of large-scale vortices behind the dish, which in turn influence the local circulations in the vicinity of the receiver. For  $i=90$  deg, i.e. head-on wind, vortices behind the dish cause the low magnitude air flow toward the aperture plane. On the other hand, for  $i=45$  deg, there occurs a large circulation encompassing the receiver, which induces stronger tangential flow at the aperture plane.

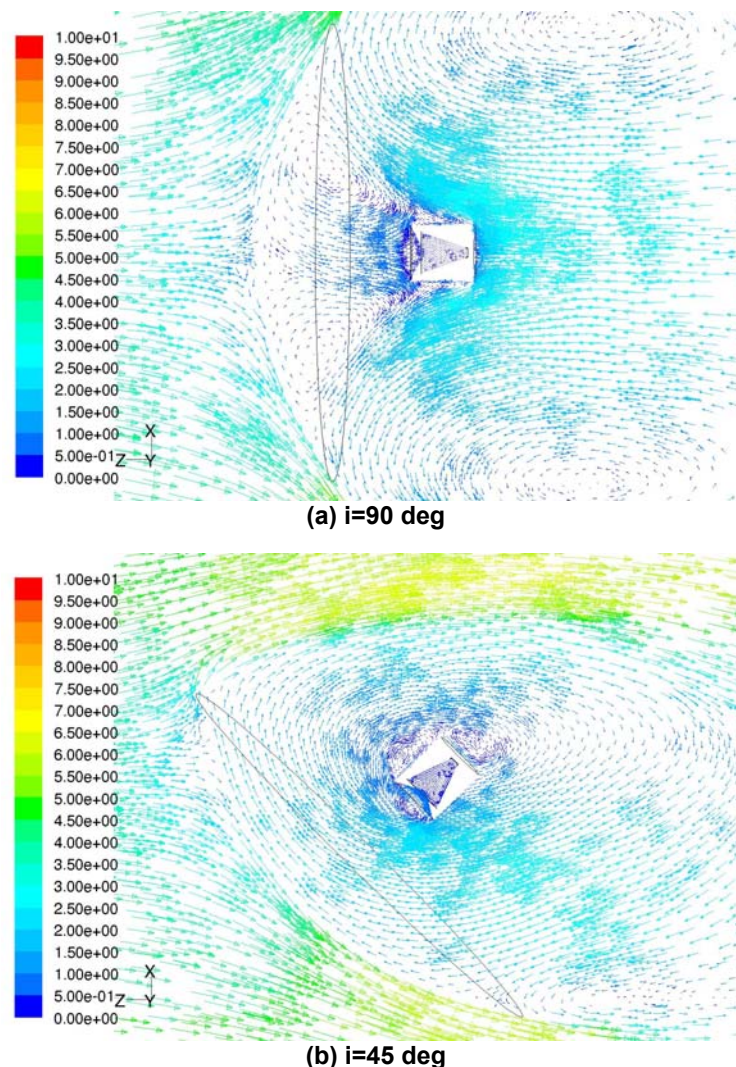
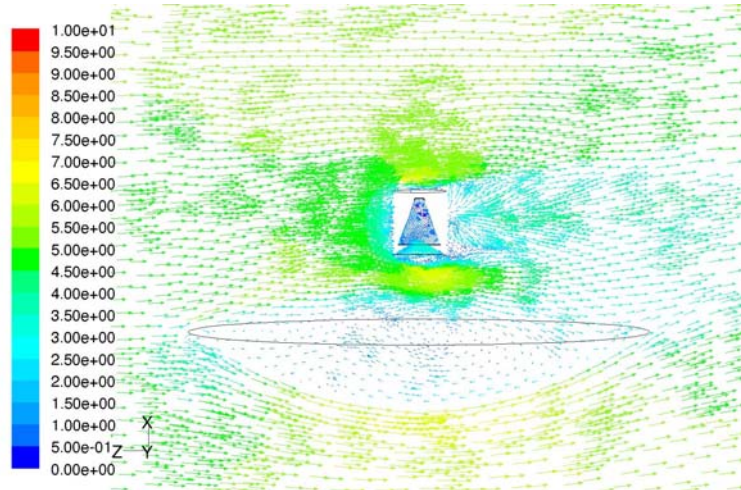
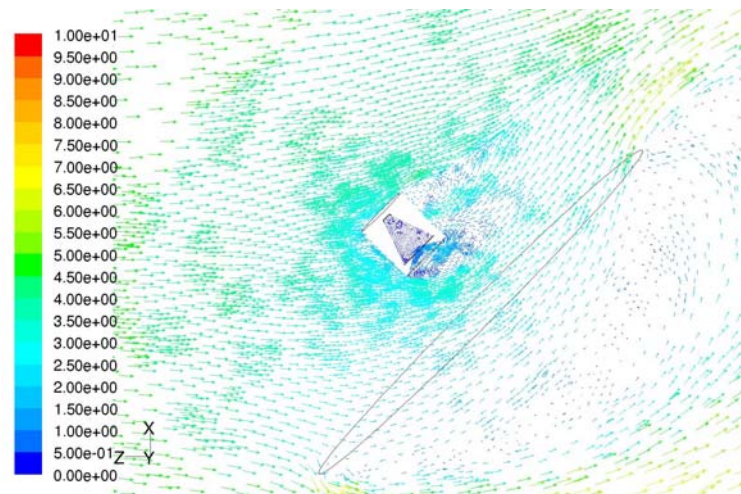


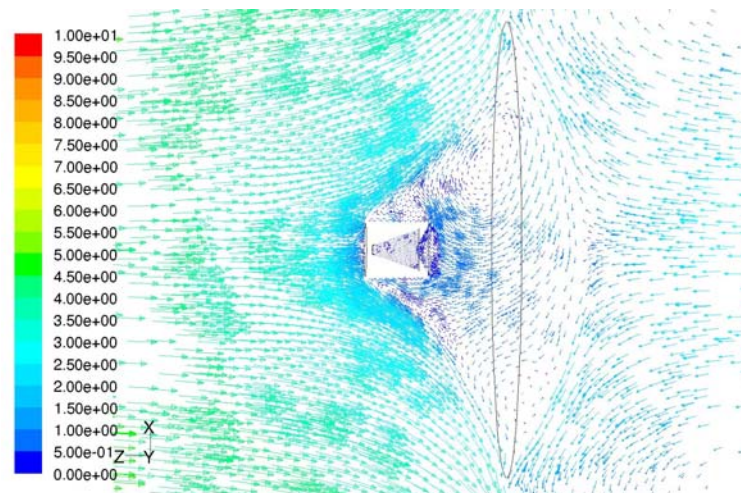
Figure 3 Velocity Vector Field (m/s) for the Case of Freestream Wind Speed  $V_\infty = 5$  m/s.



(c)  $i = 0$  deg



(d)  $i = -45$  deg



(e)  $i = -90$  deg

Figure 3 (cont.) Velocity Vector Field (m/s) for the Case of Freestream Wind Speed  $V_\infty = 5$  m/s.

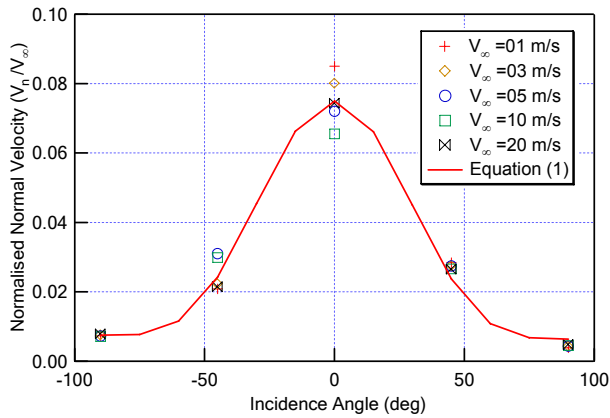


**Figure 4 Normal Velocity Magnitude.**

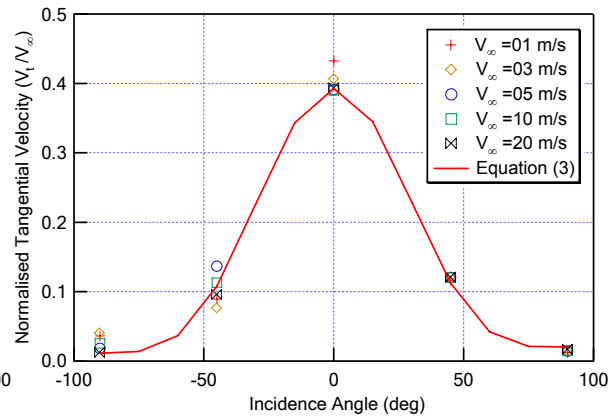


**Figure 5 Tangential Velocity Magnitude.**

For  $i \leq 0$  deg, it is obvious that local circulations in the vicinity of the receiver are generated by an interaction between the wind and the receiver itself. It can be observed that, for  $i=0$  and  $-45$  deg, the flows near the aperture are essentially dominated by the tangential components as similar to the case of  $i=45$  deg.

For  $i=-90$  deg, the pattern of the flow between the receiver and the dish is virtually similar to that of the case of  $i=90$  deg. The receiver aperture is situated in the low-velocity stagnation zone, in which vortices induce the low-magnitude flow toward the cavity.

Figures 4 and 5 show the resulting normal and tangential velocity magnitudes at the aperture plane normalised by the freestream velocity, respectively. It is obvious that there is a similarity in the variations of both components with wind speeds and incidence angles, but with the larger magnitude for the tangential one. Both components show the peaks at  $i=0$  deg and decrease toward  $i=-90$  deg and  $i=90$  deg. Interestingly, they are virtually symmetrical in respect of the incidence angle despite the fact that the corresponding geometry of the system are not indeed symmetrical, i.e., wind incident at the back of the receiver for  $i=-90$  deg, while wind incident at the back of the dish for  $i=90$  deg (cf. Figures 1b and 3).

At freestream velocity  $V_\infty$  of 20 m/s, the maximum normal component of the local wind is 1.5 m/s at  $i=0$  deg, while the maximum tangential component is 7.9 m/s, which corresponds to 7.5% and 40% of the freestream wind speed as shown in Figures 4 and 5, respectively. Except for  $i=0$  deg, the velocity magnitudes for other incidence angles are lower than  $\sim 0.5$  m/s for the normal component and  $\sim 3$  m/s for the tangential component. This is confirmed by in-situ measurements of the actual system, which were carried out on some windy days with the use of a turbine wind meter. The measurement was made at various azimuthal positions of the dish. It was found that the wind speed at the aperture plane rarely exceeded 2 m/s, while the maximum freestream wind velocity ever recorded was approximately 6 m/s.

From the above results, the normal wind speed at the aperture plane  $V_n$  has been correlated to the freestream wind speed  $V_\infty$  by the following equation:

$$V_n = C_n \cdot V_\infty, \quad (1)$$

where  $C_n$  is a function of the wind incidence angle  $i$ :

$$C_n = 0.006934 - 0.0003546 \cdot i + 0.06806 \cos(i)^4, \quad (2)$$

In the similar manner, the correlation for the parallel wind speed at the aperture plane  $V_t$  can be written as:

$$V_t = C_t \cdot V_\infty, \quad (3)$$

where  $C_t$  is:

$$C_t = 0.01581 + 0.002784 \cdot i + 0.3771 \cos(i)^4, \quad (4)$$

where  $i$  is in radian.

Equations (1) and (3) are shown as solid lines in Figures 4 and 5, respectively, which indicate that the equations fit the data well. At  $i=0$  deg, the maximum deviations are approximately 15% for the normal velocity and 9% for the tangential velocity. Though the deviation of both components can be as high as 70% at  $i=-90$  deg and  $i=90$  deg, due to the fact that their absolute magnitudes are small at those incidence angles. The similarity of the functions for the normal and parallel components is remarkable. This further indicates their similar dependency on the speed and the direction of freestream wind.

As obviously shown in the results, the presence of a large obstacle, i.e. the dish, results in the drastic reduction of the normal component at the receiver aperture. It is found that the ratio of the normal to the parallel components is less than 20% in most cases, but can be as high as 66% for the case of  $i=-90$  deg and  $V_\infty=20$  m/s. Nonetheless, the magnitudes of both components are significantly low at that incidence angle.

Considering that the local wind is predominately parallel, together with the fact that the parallel wind yields the greater increase of the convection heat loss than the normal wind as mentioned earlier in the previous work, e.g. in Ma (1993), it should be possible to simplify the combined convection loss prediction by taking into account only the parallel component.

Accordingly, Equation (3) can be employed to estimate the magnitude of the parallel wind at the aperture plane to be used in conjunction with a combined convection correlation for convection loss prediction. The covered range of freestream wind speed is  $0 \text{ m/s} \leq V_\infty \leq 20 \text{ m/s}$ . Note that Equation (3) should also be applicable to the dish at other inclinations other than horizontal position, because the present simulations were undertaken regardless of the gravitational effect which is only crucial for the buoyancy-driven free convection. Therefore, in this case, the incidence angle  $i$  can be generalised as:

$$i = \theta - 90 \text{ deg}, \quad (5)$$

where  $\theta$  is the angle between freestream wind vector and the outward normal vector of the aperture plane. It should be noted that, however, the combined convection correlation should take into account the relevant direction of the local wind that might either oppose or promote the buoyancy flow.

It is found that for  $i=90$  deg and  $-90$  deg, the relevant direction of the parallel wind is not well-defined. That is because the flow is not steady and the direction changes periodically as time progresses. On the other hand, for  $i = 45$  deg,  $0$  deg, and  $-45$  deg, the relevant direction of the parallel wind can be determined as illustrated in Figure 6. It is this direction that needs to be considered by the loss model. If the direction of the wind is opposite to that of the buoyancy flow then the two effects combine destructively, whereas it is constructive if both flows are in the same direction or perpendicular to each

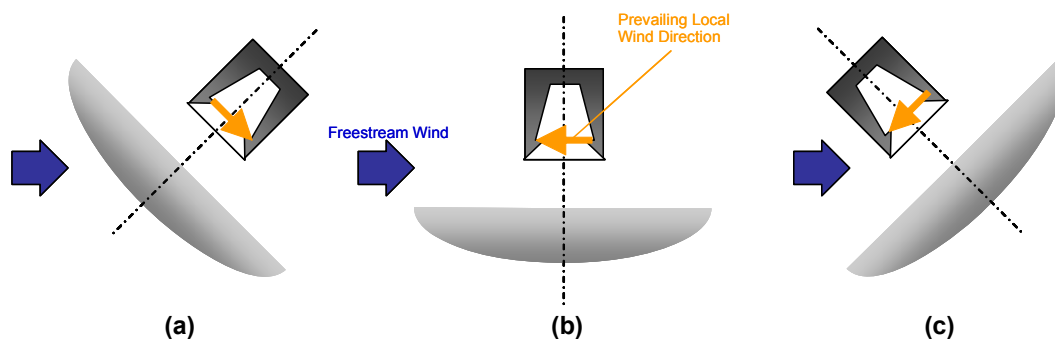


Figure 6 Prevailing Local Wind Direction at the Aperture Plane: (a)  $i=45$  deg, (b)  $i=0$  deg, and (c)  $i= -45$  deg.

other.

Lastly, it should be noted that the complicated velocity pattern results from the interaction of the flow with the dish and receiver structures and so should be subject to the particular dish-receiver configuration considered herein. Hence, one should bear in mind that the present result might not be applicable for other dish-receiver configurations.

#### 4. CONCLUSIONS

The numerical simulation was carried out in order to investigate the local wind characteristics at the receiver aperture with a presence of the paraboloidal dish. It is found that the local wind speed at the aperture is the largest when the freestream wind is parallel to the aperture plane, and virtually shows the symmetrical behaviour in respect of the incidence angle.

The tangential component of the local wind is found to be dominant in most cases. Therefore, for the first approximation to a combined convection loss model, the wind at the aperture plane can be assumed parallel, and its magnitude varies with the incidence angle of the freestream wind.

#### 5. REFERENCES

- Fluent Inc. (2002), *Fluent 6.0 User Guide*.
- Ma R. Y. (1993), *Wind Effects on Convective Heat Loss from a Cavity Receiver for a Parabolic Concentrating Solar Collector*, Contractor Report SAND92-7293, Sandia National Laboratories, USA.
- Paitoonsurikarn S., Lovegrove K. (2003), *On the study of Convection Loss from Open Cavity Receivers in Solar Paraboloidal Dish Application*, Proceeding of Solar 2003, ANZSES Annual Conference 2003, Melbourne, Australia.
- Paitoonsurikarn S., Taumoefolau T., and Lovegrove K. (2004), *Estimation of Convection Loss from Paraboloidal Dish Cavity Receivers*, Proceedings of 42<sup>nd</sup> ANZSES Conference, 28 November - 1 December 2004, Perth, Australia.
- Taumoefolau T. (2004), *Experimental Investigation of Convection Loss from a Model Solar Concentrator Cavity Receiver*, Master Thesis, Department of Engineering, ANU, Canberra, Australia.
- Taumoefolau T., Paitoonsurikarn S., Hughes G., and Lovegrove K. (2004), *Experimental Investigation of Natural Convection Heat Loss from a Model Solar Concentrator Cavity Receiver*, J. Sol. Eng. 126, 801-807.